Published in final edited form as:
ACS Nano. 2011 July 26; 5(7): 5408–5416. doi:10.1021/nn200489j.

Biomimetic Chemical Sensors Using Nanoelectronic Readout of Olfactory Receptor Proteins

Brett R. Goldsmith[†], **Joseph J. Mitala Jr.**[‡,§], **Jesusa Josue**[⊥], **Ana Castro**[‖], **Mitchell B. Lerner**[†], **Timothy H. Bayburt**[#], **Samuel M. Khamis**[Δ], **Ryan A. Jones**[Δ], **Joseph G. Brand**[⊥], **Stephen G. Sligar**[#], **Charles W. Luetje**[‖], **Alan Gelperin**[⊥,▽], **Paul A. Rhodes**[Δ,¶], **Bohdana M. Discher**[‡,§], and **A. T. Charlie Johnson**[†,‡,*]

[†]Department of Physics & Astronomy, University of Pennsylvania, Philadelphia, Pennsylvania 19104, United States

[‡]Nano/Bio Interface Center, University of Pennsylvania, Philadelphia, Pennsylvania 19104, United States

[§]Department of Biochemistry and Biophysics, University of Pennsylvania, Philadelphia, Pennsylvania 19104, United States

[⊥]Monell Chemical Senses Center, Philadelphia, Pennsylvania 19104, United States

[‖]Department of Molecular and Cellular Pharmacology, University of Miami, Miami, Florida 33101, United States

[#]Department of Biochemistry, University of Illinois, Urbana, Illinois 61801, United States

[Δ]Nanosense, Inc., Redwood City, California 94063, United States

[▽]Princeton Neuroscience Institute, Department of Molecular Biology, Princeton University, Princeton, New Jersey 08544, United States

[¶]Evolved Machines, LLC, Palo Alto, California 94301, United States

Abstract

We have designed and implemented a practical nanoelectronic interface to G-protein coupled receptors (GPCRs), a large family of membrane proteins whose roles in the detection of molecules outside eukaryotic cells make them important pharmaceutical targets. Specifically, we have coupled olfactory receptor proteins (ORs) with carbon nanotube transistors. The resulting devices transduce signals associated with odorant binding to ORs in the gas phase under ambient conditions and show responses that are in excellent agreement with results from established assays for OR–ligand binding. The work represents significant progress on a path toward a bioelectronic

[*]Address correspondence to cjohnson@physics.upenn.edu.

Supporting Information Available: Information concerning chemical functionalization of carbon nanotube devices. Western blot analysis of receptor purification. Additional data on odorant responses of mOR-NT devices. Control experiment to determine the response time of the measurement apparatus. Experiment with an array of mOR-NT devices. This information is available free of charge *via* the Internet at http://pubs.acs.org.

nose that can be directly compared to biological olfactory systems as well as a general method for the study of GPCR function in multiple domains using electronic readout.

Keywords

bioelectronics; vapor sensor; olfactory receptor proteins; field effect transistor; nanotube

Integration of modern nanoelectronic technology with the potent molecular machines of living organisms offers a pathway to advanced chemical sensing modalities and high-throughput screening of ligand binding. While significant progress has been made along this path using soluble proteins[1–4] and nucleic acids,[5–7] integration of amphiphilic membrane proteins remains in an early state of development[8–10] despite their vital and varied functionality in living organisms. G-Protein coupled receptors (GPCRs) are a very large family of transmembrane receptors that recognize molecules in the intercellular region and activate important signal transduction pathways. They are involved in many diseases and are important targets for modern drug agents. Olfactory receptor proteins (ORs) are the most numerous class of GPCRs, representing transcription products of ~3% of the mammalian genome.[11] Here we report a method to integrate ORs with carbon nanotube (NT) transistors. Our method includes the formation of a direct chemical bond that localizes the OR within nanometers of the NT device, in contrast to earlier work, where (mobile) membrane proteins were incorporated into a macroscopic lipid bilayer covering the NT transistor. Because of this, we enable direct readout of OR–ligand binding by the NT device.

Efforts to interface nanoelectronic devices to membrane proteins confront challenges due to the hydrophobic nature of their transmembrane domains, which complicates their expression, purification, and solubilization.[12–14] In this work, ORs were purified from cells and then solubilized in two distinct nanoscale constructs: digitonin micelles[12] and engineered, stable, self-assembling nanoscale membrane assemblies known as “nanodiscs”.[15] Solubilized ORs were attached *via* a polyhistidine tag (Histag) to high-quality NT transistors that were previously functionalized with nickel-nitrilotriacetic acid (Ni-NTA).[16]

These advancements in the purification, packaging, and integration of membrane proteins lead to striking improvements in the practical qualities of membrane protein-enabled bioelectronics. This is most dramatically shown in the stability and longevity of the devices, which have demonstrated useful and repeatable sensor functionality over months, instead of the usual day-long, single-experiment lifetime that greatly limits potential applications of current bioelectronics. The use of polyhistidine tags and artificial membrane constructs allows precise orientation of the properly folded biological component relative to the transistor readout element. The OR-NT devices detect vapor analytes under ambient conditions, with sensor responses that are reversible, repeatable, and durable. This work thus represents a significant advance beyond earlier reports where membrane proteins coupled to electronic devices were housed in crude membrane fractions[17] or attached to fusion proteins.[18]

Three mouse olfactory receptor proteins (mORs) were selected for overexpression and integration with NT transistors for vapor response testing against a panel of eight odorants: mOR174-9 (also known as mOR-EG) is known to respond to eugenol;[19] mOR203-1 and mOR256-17 respond to 2-heptanone and cyclohexanone, respectively.[20] Two of these mORs (174-9 and 256-17) were screened with a panel of eight odorants using a *Xenopus* oocyte expression system in combination with robotic electrophysiology.[21] The third mOR (203-1) did not express well in the *Xenopus* oocytes; however similar information is available from expression in human embryonic kidney (HEK) cells from others.[20] Table 1 summarizes response characteristics of the three mORs when expressed in heterologous surrogates and also when coupled to the electronic system described in this paper. The response characteristics of ORs are known to be broadly tuned, so that individual ORs recognize a range of different odorants with varying degrees of specificity.[22]

Recombinant mORs were expressed with an N-terminal His-tag in Sf9 insect cells to simplify the purification and guide the attachment of ORs to carbon nanotube devices.[13] After harvesting the cells, target mORs were purified using magnetic beads treated with Ni-NTA. The presence and correct molecular weight of the protein after the purification was verified by Western blot (see Supporting Information). Throughout all stages of the purification process, the protein was maintained in ~4.88 mM (0.6% w/v) digitonin, a surfactant containing a cholesterol-like backbone that promotes functional solubilization of membrane proteins.[12] At concentrations above 0.5 mM, digitonin forms micelles that can house and solubilize individual ORs in a membrane-like environment. In a second approach, ORs were embedded in soluble “nanodiscs”, disk-shaped protein–lipid particles designed to self-assemble with well-controlled size and composition.[15,23] Consistent with previous accounts of nanodisc behavior,[24] mOR-nanodiscs exhibited significantly enhanced stability in solution, with a shelf life of several months. In contrast, digitonin-solubilized mORs would aggregate within hours, as confirmed by dynamic light scattering measurements (data not shown); therefore these solutions were used to functionalize NT devices immediately after purification.

Three-terminal transistor circuits that acted as readout elements of OR–odorant binding were fabricated from carbon nanotubes grown on oxidized silicon substrates by catalytic chemical vapor deposition as described previously.[5] Device current–gate voltage (I–V_G) characteristics were measured under ambient laboratory conditions, and circuits with an on/off ratio exceeding 1000 were selected for use in experiments. Devices were functionalized with carboxylated diazonium salts, which readily form covalent bonds to NTs.[25] As detailed in Materials and Methods, a mild diazonium treatment was used, since excessive covalent modification of NTs destroys the semiconducting properties necessary for efficient signal transduction.[16,25] The carboxylic acid functionality of the diazonium salt was activated with 1-ethyl-3-[3-dimethylaminopropyl]carbodiimide hydrochloride/sulfo-*N*-hydroxysuccinimide (EDC/sNHS) treatment, followed by attachment of the NTA linker. This treatment provides ~5–10 attachment sites for each 1 μm length of exposed nanotube (Figure 1a). Device fabrication was completed with the addition of Ni ions, which are chelated by the NTA complex, and incubation in a solution of mOR-containing digitonin

micelles or nanodiscs. This treatment allowed the His-tagged proteins to associate with the Ni-NTA attachment sites. Figure 1b is a schematic of the finished device.

We conducted numerous control experiments using identical incubation and washing protocols to confirm that binding between mORs and the nanotube was controlled by the Ni-NTA:His-tag interaction. We confirmed that empty digitonin micelles and empty nanodiscs have no affinity for Ni-NTA-modified nanotubes. We exposed Ni-NTA-functionalized devices to proteins *without* His-tags and confirmed that no bound proteins remain after the wash protocol. The proteins for the latter experiments were commercially obtained protein G; we did not use the mORs since they were not designed for His-tag removal. All control experiments are thus consistent with the hypothesis of (oriented) protein attachment *via* the expected chemical bond between the Ni-NTA-functionalized nanotube and the protein's His-tag.

Current–gate voltage (I–V_G) characteristics were used to monitor the effect of chemical functionalization on performance characteristics of nanotube transistors.[2–5] Figure 1c shows a typical I–V_G curve of an as-fabricated device and its evolution through the functionalization process. We assume that the mechanism underlying changes in NT conduction is dominated by electrostatic coupling to the local environment. Shifts in threshold gate voltage for conduction are attributed to changes in the charge in NT environment, while variation in the on-state current is assumed to reflect changes in carrier scattering. Ni-NTA functionalization leads to a ~3-fold decrease in the on-state current of the NT, which is ascribed to carrier scattering due to covalent attachment of the complex to the NT sidewall. The observed threshold voltage shift of −1 V (from ~10 V to ~9 V) indicates that Ni-NTA functionalization leads to increased positive charge in the nanotube environment, which is associated with the 2+ charge of the nickel ions. Addition of mOR-micelles results in a pronounced decrease in the on-state current and a strong negative shift of the threshold voltage, both consistent with earlier work on protein-functionalized NT transistors.[1–3,14] Similar shifts in threshold and resistance are seen for devices functionalized with mOR-nanodisc constructs.

Responses of NT devices to odorant exposure were measured in a sealed environmental test system through which gas flows of known odorant concentrations were passed (see Materials and Methods). High-purity nitrogen served as a carrier gas for the odorants and to flush the device between exposures to odorant-containing flows. A humidified environment was found to be necessary for device stability, so water vapor was added to all flows to create a relative humidity (RH) of 50%. Devices under test were loaded into the chamber and allowed to equilibrate in a flow of nitrogen at 50% RH. The device was put into the hole conduction regime by setting the back gate voltage 3 V below the threshold voltage, and the dc resistance was monitored as the device was exposed to gas flows containing odorants for 100 s and then 50% RH nitrogen for 100 s. Five cycles of odorant and carrier gas were used at each odorant concentration to quantify response reproducibility. The response is reported as a fractional change in dc current at constant bias voltage. In NT transistors, changes in resistance due to chemical interactions are caused by shifts in electron scattering or in the effective gating of the transistor, both of which are likely to occur in the odorant–protein–nanotube system.[2,14,26]

Characteristics of odorant responses of mOR-functionalized devices are shown in Figure 2. Large positive responses to eugenol are observed (*i.e.*, increase in device current; Figure 2a,b), consistent with strong responses observed in *Xenopus* oocytes expressing the same OR. NT devices have rapid and reproducible responses and full recovery to baseline, both on second time scales (Figure 2c). As is true for ORs *in vivo*, refreshing the device requires only flushing the odorant from the chamber with carrier gas. As found in previous work with NT-based vapor sensors,[5] differences in device properties can be normalized by presenting sensor responses as a percent change from the baseline current (% $\Delta I/I$). This normalization corrects for device-to-device variation as well as slow drift in a single device over several days (Figure 2b).

After fabrication, micelle devices remained active with stable normalized responses for ~5 days when stored in a humid environment. Devices then became fully inactive and displayed no response to odorant vapors, as was typical of unfunctionalized NT devices (see Table 1). We interpret this degradation as indicative of a breakdown of the digitonin micelle, causing the OR to denature and lose its distinctive odorant-binding properties. In contrast, nanodisc-functionalized devices stored in a humid environment showed ~25% reduction in normalized odorant response over the first several days, but at this point the device responses stabilized with very long lifetimes. Devices showed reproducible responses for longer than one month, with one device maintaining mOR-specific responses to odorants for 10 weeks (Figure 2c). We interpret this result as implying that the nanodisc construct provided a relatively stable environment for the OR, with only minor degradation over the first few days.

We used a high-speed data acquisition system to investigate the shape and timing of device responses (Figure 2d). We found that response and recovery data are well fit by double-exponential functions (blue lines in Figure 2c), with significant response on time scales < 10 s. The observed time scales are intrinsic to the mOR-NT system, since control experiments indicated that the response time of the apparatus itself is less than 100 ms (Supplemental Figure 4). Response and recovery time scales show little variation with mOR identity, or whether digitonin micelles or nanodiscs were used to solubilize the ORs. Response and recovery are significantly faster than found in heterologous measurements, where a signal transduction pathway is used to report receptor activation, and responses often take several hundreds of seconds.[21]

Responses of OR-functionalized devices were measured for a range of odorants and odorant concentrations. Multiple devices (2–5) were tested for each OR, and the results combined to generate the responses and statistical errors reported in Table 1. Figure 3a shows the concentration dependence of the response of NT devices functionalized with mOR203-1 in digitonin micelles to several odorants, while Figure 3b provides representative examples of how device responses varied with concentration, odorant, and mOR identity. To account for different vapor pressures of the odorants, concentrations are quantified as a fraction of the saturated vapor. Figure 3a shows substantial agreement between the NT device measurements and the HEK data for this mOR, for example, the strong response to 2-heptanone and lack of response to heptanal and acetophenone. Interestingly, the NT device shows nearly identical responses to the chemically similar odorants 2-heptanone and *n*-amyl

acetate. The molecules differ only by a single oxygen atom in the functional group attached to a five-carbon chain, and they are perceived as nearly identical by humans.[27] In mice, these two chemicals produce identical neural excitations[28] and olfactory responses,[29] although the interaction of *n*-amyl acetate with the particular mOR 203-1 has not been measured previously. In other cases, odorants with related molecular structures elicit very distinct responses. For example, three odorants in Figure 3a share a carbon ring motif (eugenol, acetophenone, and cyclohexanone), but the odorant responses differ substantially (positive, zero, and negative, respectively).

Similar to other NT-based molecular detection systems, our current understanding of the response mechanism is primarily qualitative. The functionalization chemistry results in the localization of OR-specific binding pockets at distances of a few nanometers from the NT, with a nanoscale hydration layer provided by the humid atmosphere. When odorant molecules are solvated by the hydration layer and bound in the pocket, the conductance of the NT devices is altered, which we assume reflects changes in carrier density and carrier scattering associated with the electrostatic potential at the NT sidewall. These changes can occur even for the case of uncharged odorant molecules, as is also reported for other sorts of functionalized NT devices.

Of the eight odorants tested, only 2,4-dinitrotoluene is not found in nature. It also produces a response at the lowest concentrations, ~7 ppb, in the range of a “moderately potent” detection threshold for an OR.[30] It is not known whether mice can detect dinitrotoluenes, but there is strong evidence suggesting that they can be sensed by bomb-detecting dogs and rats.[31,32] Mammalian olfactory systems have the ability to detect and categorize new odorants, even those not present during the evolutionary history of the organism, a feature beyond the capability of man-made chemical sensor systems.[22] Our results suggest that the capacity of mORs to bind to nonbiological odorants is preserved when integrated with NT devices, maintaining the mOR's ability to adapt to new analytes. This system thus has potential for the creation of chemical sensor arrays that would have the flexibility of the biological sense of smell; fabrication of such arrays using existing lithography and liquid spotting methods has already been demonstrated (Supplemental Figure 5).

The data indicate that mOR-NT devices have characteristics that are typical of functional ORs *in vivo*, such as the need for a humid environment, the relatively short lifetime of the devices, and the odorant response timing. The data summarized in Table 1 indicate that mOR-NT device responses to odorants show broad agreement with mOR odorant responses found using heterologous techniques for two of the three mORs tested, with only mOR 256-17 showing significant disagreement. Neither the NT nor heterologous systems duplicate the *in vivo* OR response exactly, but areas of agreement between these two test systems strengthen the interpretation of select sensitivities as present in the natural host.

The responses of the devices and the heterologous systems show considerable agreement, although discrepancies exist. For mOR 174-9 and mOR 203-1, all disagreements consist of strong response by the NT device and weak or no response in the heterologous system. Since the NT device responds to all molecules that bind near it, this could reflect odorant binding to the mOR that elicits no cellular response (*e.g.*, an antagonist) or possibly odorant

binding not to the mOR but instead to the NT or the digitonin micelle (or nanodisc) that encapsulates the mOR. To exclude the latter possibilities, we conducted control experiments on bare NT transistors and on devices treated with Ni-NTA and empty digitonin micelles (*i.e*., no mOR; see Table 1). We observed no significant response to any of the tested odorants, with the exception of a small response to cyclohexanone. We infer that observed device responses reflect NT transistor readout of the binding affinity of the attached mORs, with the possible exception of cyclohexanone. This reasoning informs the interpretation of the data for mOR256-17, which shows the broadest set of responses in the heterologous system and poor agreement between the NT and heterologous data. The synthetic membrane environments that we used to house the OR may lead to subtle perturbations to the mOR structure, thereby shuffling the multiple affinities that characterize mOR256-17.

In conclusion, we have successfully developed purification, solubilization, and biofunctionalization schemes that enable control of the bionano interface between olfactory receptor (membrane) proteins and carbon nanotubes. Vapor response measurements demonstrate that ORs with known odorant sensing properties can be coupled to an electronic device and transfer many of those sensing properties to the device. Future work exploring additional ORs and other types of GPCRs could help to understand differences between protein–nanotube measurements, heterologous measurements, and *in vivo* measurements. Conceptually, this opens up a very large domain of intra- and intercellular communication to electronic eavesdropping and could serve as a powerful tool for molecular and cell biology research.

MATERIALS AND METHODS

Electrophysiological Characterization of Mouse Olfactory Receptors Expressed in *Xenopus* Oocytes

We refer to mORs using the nomenclature of Zhang and Firestein.[33] Receptor coding regions were cloned into the pCI expression vector (Promega) containing an N-terminal extension consisting of the N-terminal 20 amino acid residues of human rhodopsin. Receptors were co-expressed with human Ga_{olf} and the human cystic fibrosis transmembrane regulator (CFTR), serving as a reporter channel.

Oocytes were surgically removed from mature *Xenopus laevis* frogs (Nasco). Follicle cells were removed by treatment with collagenase B (Boehringer Mannhem) for 2 h at room temperature. Oocytes were injected with cRNA in 23 nL of water. cRNA quantities injected per oocyte: mORs, 25 ng; Ga_{olf}, 10 ng, CFTR, 1 ng. Oocytes were incubated at 18 °C in Barth's saline (in mM: 88 NaCl, 1 KCl, 2.4 $NaHCO_3$, 0.3 $CaNO_3$, 0.41 $CaCl_2$, 0.82 $MgSO_4$, 15 HEPES, pH 7.5 and 12 μg/mL tetracycline) for 2–4 days prior to electrophysiological recording.

Odorant-induced Cl^- currents, resulting from cAMP-mediated activation of the co-expressed CFTR reporter channel, were measured 2–4 days after cRNA injection using a two-electrode voltage clamp in an automated parallel electrophysiology system (OpusExpress 6000A, Molecular Devices). Oocytes were perfused with ND96 (96 mM NaCl, 2 mM KCl, 1 mM $CaCl_2$, 1 mM $MgCl_2$, 5 mM HEPES, pH 7.5). Micropipets were filled with 3 M KCl and

had resistances of 0.2–2.0 MΩ. The holding potential was −70 mV. Current responses, filtered (4-pole, Bessel, low pass) at 20 Hz (−3 db) and sampled at 100 Hz, were captured and stored using OpusXpress 1.1 software (Molecular Devices). Analysis was done using Clampfit 9.1 software (Molecular Devices).

Our electrophysiological results for mOR256-17 are at some variance with published reports[20] that mOR256-17 responds to cyclohexanone, but not to heptanal or 2-heptanone. We obtained the mOR256-17 expression construct from the Matsunami laboratory[20] and found that, in our hands, this construct yields results in agreement with what we show in Figure 1 in this paper. Similarly, when the Matsunami laboratory retested their mOR256-17 expression construct in their assay system, they obtained results in agreement with our results (Dr. Hiroaki Matsunami, personal communication).

Mouse Olfactory Receptor Expression in SF9 Cells

a. mOR 174-9 and mOR 203-1—Recombinant mouse olfactory receptors (mOR) 174-9 and 203-1 were expressed in an Sf9 insect cell system using the BaculoDirect Expression System (Invitrogen). The entry clones for mOR 174-9 (Olfr73; BC141607) and 203-1 (Olfr992; BC141642) were from Invitrogen. The DNA sequence of each receptor was verified using primer pairs specific to each receptor. The DNA sequences of both mOR 174-9 and mOR 203-1 clones were verified using GW1 forward primer (GTTGCA-ACAAATTGATGAGCAATGC) and GW2 reverse primer (GTTGC-AACAAATTGATGAGCAATTA).

The entry clones were used to create an expression clone for each mOR through linear recombination reaction using BaculoDirect Linear DNA with an N-terminal His-tag. Two recombinant expression clones were created: mOR 174-9 with N-terminal His-tag, and mOR 203-1 with N-terminal His-tag. All expression clones were used individually to transfect Sf9 insect cells. Six days after transfection, the cells demonstrated signs of infectivity. The viral stock was collected and was labeled P1 viral stock. The P1 viral stock was stored at ~80 °C in the dark with 10% fetal bovine serum (FBS) to protect the recombinant virus from proteases. Second and third rounds of viral amplification were performed and labeled P2 and P3 viral stocks, respectively. An aliquot of P3 viral stock was collected and used to isolate and purify the viral DNA for PCR to check the orientation of the mOR DNA fragment after transfection and expression.

The viral titer of all P3 viral stocks was determined following the protocol on the BacPAK Baculovirus Rapid Titer Kit (Clontech). Once the viral titer was known, Baculovirus Infected Insect Cell (BIIC) stock was prepared for each recombinant mOR. BIIC stock was found to be more stable than the viral stock. BIIC stock with a multiplicity of infection (MOI) of 3 was prepared on the basis of existing methodology.[34] Sf9 cell cultures were infected with BIIC stock to express the recombinant mORs. The expression of all recombinant mORs was monitored by determining the percent viability, total cell density, and viable cell density during the infection process. A decrease in percent viability and increase in both the cell diameter and viral titer can be observed during infection. While still in their log growth phase state, the cells were harvested, as the percent viability of the Sf9 culture reached 70–80%. Cells were harvested by centrifugation (1000g, 10 min, 4 °C).

b. mOR 256-17—moR256-17 clone was placed in frame into pFastBac HT (Invitrogen) between *Eco*RI and *Not*I using common procedures for SF9 insect cells.[35] Colonies were screened by PCR. Virus was generated using the Bac-to-Bac system (Invitrogen) according to the manufacturer's instructions. Virus was quantified by plaque assay. For protein production cells were grown in shaker flasks at 125 rpm at 27 °C either in Grace's supplemented medium with 10% FBS or in SF900II medium with 2% FBS. Media also contained 0.25 mg/L amphotericin B (Sigma A9528), 20 mg/L gentamicin (Gibco 15750-060), and 0.1% Pluronic F-68 (Sigma P5556). Cells were infected at a MOI of 1 at a cell density of (1–2) × 10^6 cells/mL. Cells were harvested 48 h post-infection, weighed, frozen in liquid nitrogen, and stored at −80 °C. Expression was confirmed by Western blot using antipentahistidine primary antibody (Qiagen).

Purification of mORs for Incorporation into Digitonin Micelles

a. Preparation of the Crude Plasma Membrane Fraction (CMF—Cell pellets were washed initially by resuspending in a concentration of phosphate-buffered saline (PBS) equivalent to the osmolality of the cell growth media and centrifuged (1000*g*, 10 min, 4 °C). The pellets were resuspended in a lysis buffer consisting of 20 mM Tris-HCl (pH 8.0), 1 mM EDTA, 1 mM EGTA, 0.4% (v/v) ethanol, 0.1 mM phenylmethanesulfonyl fluoride, and protease inhibitor cocktail designed for Sf9 cells (Sigma) and homogenized with a Dounce homogenizer (pestle A, 0.0030–0.0060 in.). In some cases, such as when there was a large amount of nuclei present in the homogenate (as evident from the presence of a clear jelly-like substance), the homogenized cell suspension was centrifuged (300*g*, 10 min, 4 °C) to remove the more dense nuclei and unbroken cells. The homogenate, or supernatant in the case of the latter, was then centrifuged (40000*g*, 20 min, 4 °C) and the supernatant discarded. The pellets were resuspended in a solution of 20 mM Tris-HCl (pH 8.0), 3 mM $MgCl_2$, 0.5 mM $CaCl_2$, and 10 μg/mL deoxyribonuclease (DNase)-I and centrifuged (40000*g*, 20 min, 4 °C). The supernatant was discarded, and the pellet was resuspended in approximately 400 μL of 20 mM Tris-HCl (pH 8.0), 3 mM $MgCl_2$, 0.5 mM $CaCl_2$, and 10 μg/mL DNase-I per 30 mL of cells harvested (ca. 0.75 mg total protein/mL cells harvested), using a 5 mL Wheaton homogenizer. Resuspended pellets were then aliquoted into Eppendorf tubes, flash frozen in liquid nitrogen, and stored at −80 °C.

b. mOR Purification Using Nickel-Magnetic Beads—A 400 μL aliquot of CMF was solubilized in a solution such that its final composition was 6.76 mM digitonin, 19 mM NaH_2PO_4, 115 mM NaCl, 12 mM Tris, 2 mM $MgCl_2$, 0.3 mM $CaCl_2$, and 6.2 μg/mL DNase-I. Solubilization of the CMF was achieved *via* agitation on a benchtop vertical rotator for 1 h or *via* sonication with a microtip (Misonix Ultrasonic Liquid Processor). PureProteome nickel-magnetic beads (Millipore) were added to the solubilized CMF in a volume of 50 mM NaH_2PO_4 and 300 mM NaCl, pH 8.0, such that the final concentration of digitonin was 4.88 mM. The Ni-magnetic beads were mixed with solubilized CMF for 1 h at 4 °C on a vertical rotator and isolated with a magnet. The Histagged protein was eluted from the beads with approximately 1.25 mL of 4.88 mM digitonin prepared with 100 mM acetate buffer (pH 4.0), and the pH was adjusted to 8.0 using a micropH electrode. The pH adjustment typically required no more than 0.2 mL of NaOH. Note: Although the elution of the His-tagged protein from the magnetic beads was not 100% efficient, we obtained

significant amounts of protein to see it on Western blots and to perform our sensing experiments.

Purification of mORs for Incorporation into Nanodiscs

A cell pellet was thawed on ice. Cells were resuspended (2.5 mL per gram cells) in ice-cold PBS (Biowhittaker, without magnesium or calcium) containing Roche complete protease inhibitors without EDTA and Sigma inhibitor cocktail (Sigma, P8849). Cells were sonicated on ice using a Branson 450 sonifier at power 5, 80% duty cycle using a microprobe tip with eight 15 s bursts, waiting 30 s between bursts. The sample was centrifuged at 40k rpm in a Ti70 rotor at 4 °C for 30 min. Ice-cold PBS containing protease inhibitors and 2% w/v Fos-choline 12 (Anatrace) was added to the pellet, 2.5 mL per gram of cell starting material, and the sample was agitated in a Falcon tube at 4 °C for 2.5 h. The sample was then centrifuged as before and supernatant loaded onto a 5 mL nickel-chelating FF cartridge (GE Healthcare) in a cold room. The cartridge was washed with three volumes of PBS containing 20 mM imidazole (pH 7.4) and 0.4% w/v Fos-choline 12. Protein was eluted with PBS containing 500 mM imidazole (pH 7.4) and 0.4% w/v Fos-choline 12. Protein-containing fractions were pooled and protein content was measured using Coomassie Plus reagent (Pierce) with bovine serum albumin as standard.

Assembly of mOR Nanodiscs

Nanodiscs were assembled essentially as described previously.[36] Briefly, MSP1E3D1(−) without a polyhistidine tag was mixed with a 0.2 M POPC/0.4 M cholate mixture prepared as described[36] at a ratio of 140 mol POPC to one MSP1E3D1. Fos-choline 12 was added to a final concentration of 0.4%. Olfactory receptor was added to the MSP lipid mixture at a ratio of 1 mg of crude OR per 20 mg of MSP1E3D1 (MW 32 700). Protease inhibitor was added (Roche Complete without EDTA), and detergent was removed at 4 °C with overnight agitation in the presence of an equal volume of moist Amberlite XAD-2, prepared as described.[36] After removal of beads the sample was filtered using a 0.22 μm syringe filter and stored at 4 °C.

Carbon Nanotube Transistor Fabrication

Carbon nanotubes were grown on p++-doped silicon wafers (4 in. diameter) with 500 nm thermal oxide from Silicon Valley Microelectronics. Approximately 5 mL of 50 mg/L iron nitrate solution was spun onto wafers at 2000 rpm until dry to provide growth catalyst. Wafers were broken into halves and annealed at 910 °C for 15 min. Growth was performed in a 50 mm tube furnace at 910 °C in a flow of 2500 standard cubic centimeters per minute (sccm) methane and 320 sccm hydrogen with 600 sccm argon as carrier gas for 10 min. The furnace temperature was then decreased to 100 °C over approximately 2 h in a flow of 320 sccm hydrogen with 600 sccm argon before samples were removed from the furnace.

Nanotube transistor fabrication was carried out using optical lithography. Polymethylglutarimide (PMGI) (Microchem SFS2) was spun on at 4000 rpm for 45 s, and samples were baked at 150 °C for 5 min. Photoresist (Shipley 1813) was spun on at 5000 rpm for 45 s, and samples were baked at 115 °C for 1 min. After an exposure of about 100 mW/cm^2, Microposit MF-319 was used to develop devices for around 1 min.

Chrome (5 nm) and 50 nm gold were deposited in a home-built thermal evaporator. Liftoff was done in an acetone bath, followed by a bath in Microposit Remover-PG to remove the PMGI, then multiple clean water baths.

The resulting devices have a *2* μm source–drain separation. Before electrical measurement, chips were baked at 250 °C in air for 30 min to remove any polymeric residue from fabrication.

Typical nanotubes are single walled, with a diameter of 1.0–2.5 nm. Typical devices have one to three nanotubes bridging the gold electrodes. Electrical data, using the silicon wafer as a transistor back-gate, are gathered on all devices before chemical modification. Devices showing on/off ratios exceeding 1000 were selected for use in experiments.

Chemical (Ni-NTA) Modification of Carbon Nanotubes

Carbon nanotube transistors on silicon wafers were chemically functionalized using a procedure similar to that described previously.[37] All solutions were prepared using deionized water with an electrical resistance of 18.2 MΩ-cm. All chemical modifications were performed on the chips in 50 mL polypropylene Falcon tubes. First, samples were placed in a solution of 10.76 mM 4-carboxybenzene diazonium tetrafluoroborate at 45 °C for 1 h, followed by washing with acetone, methanol, and water. The chips were then placed in a solution of 2 mM EDC and 5 mM Sulfo-NHS, prepared with activation buffer (0.1 M 2-(N-morpholino)ethanesulfonic acid sodium salt, 0.5 M NaCl, pH adjusted to 6.0 with HCl) at room temperature for 15 min to activate the carboxylic acid of the 4-carboxybenzene covalently attached to the nanotubes. Immediately afterward, the chips were briefly bathed in activation buffer and placed in a solution of 11.3 mM N_{α},N_{α}-bis(carboxymethyl)-L-lysine hydrate (NTA-NH_2) prepared with PBS (0.1 M NaH_2PO_4, 0.15 M NaCl, pH adjusted to 7.35 with NaOH) for 2 h. Upon completion, the chips were washed with water and placed in a solution of 11.3 mM $NiCl_2$. After 1 h, the chips were removed from the $NiCl_2$ solution, washed with water, and stored in 25% (v/v) ethanol, at 4 °C.

Attachment of mORs to Ni-NTA-Modified Nanotubes

Chips containing Ni-NTA-modified nanotubes were removed from storage in ethanol, rinsed in water, and dried in a stream of high-purity nitrogen or argon gas. A solution containing mORs in digitonin micelles or nanodiscs, prepared as described above, was deposited on the surface of the chips for 30 min, at room temperature. A large enough volume was deposited on the chips such that any volume change over the 30 min period due to evaporation was negligible. If the solution contained surfactant-stabilized mORs, the chips were then rinsed with a 1 mM digitonin solution. If the solution contained mORs in nanodiscs, the chips were rinsed with deionized water. All samples were dried in a stream of nitrogen or argon gas (with the exception of the sample shown in Supplemental Figure 1b, which was airdried to show the CNT-micelle interaction).

Apparatus for Measuring Response of NT Devices to Odorant Vapors

The procedure for these measurements is as described in ref 38. The temperature, humidity, flow rate, and flow paths are controlled by a computer. The computer also communicates

with and controls a Keithley 6485 picoammeter that measures the current through the device. A digital acquisition card provides the 100 mV source–drain voltage and is connected to the analogue out of the Keithley 6485 to record high time resolution current data. The gate is controlled by a Keithley 617 programmable electrometer.

MKS 1179A style mass flow controllers are used to create three flows of nitrogen. One steady flow of 1000 sccm is bubbled through water to provide a humidified stream of gas. The second “sample flow” is switched between a bubbler containing the odorant being tested and a bypass that is not exposed to any odorant. The last flow serves as a “background” to further dilute the sample flow. The “sample” and “background” flows are set so that they add up to a total flow of 1000 sccm. These three flows (humidity, sample, and background) are combined and then fed into the sensing chamber. Throughout the measurement, the total flow rate, temperature, and humidity do not change.

The devices sit in a stainless steel sensing chamber, with gold pogo pin contacts to the interrogated devices. The total volume of the sensing chamber is around 40 mL. Before the measurements, tubing, fittings, valves, and the chamber are cleaned by rinsing with acetone, isopropyl alcohol, and water, followed by baking for 1 h at 150 °C.

Chemical Analytes

All odorants used are liquids under ambient conditions except for 2,4-dinitrotoluene, which is a solid. Carrier gas was bubbled through liquid odorants and forced through a column containing compressed powder of 2,4-dinitrotoluene. Analytes were used in pure form.

All odorants were purchased from Alfa Aesar except for *n*-amyl acetate, which was purchased from Sigma Aldrich.

Supplementary Material

Refer to Web version on PubMed Central for supplementary material.

Acknowledgments

This work was supported by the DARPA RealNose project. Support from the Nano/Bio Interface Center (NSF NSEC DMR08-32802) is gratefully acknowledged, as is use of its facilities. M.L. acknowledges support from the Department of Defense PCRP #PC080542P1.

REFERENCES AND NOTES

1. Star A, Gabriel JCP, Bradley K, Gruner G. Electronic Detection of Specific Protein Binding Using Nanotube FET Devices. Nano Lett. 2003; 3:459–463.
2. Zhang YB, Kanungo M, Ho AJ, Freimuth P, van der Lelie D, Chen M, Khamis SM, Datta SS, Johnson ATC, Misewich JA, Wong SS. Functionalized Carbon Nanotubes for Detecting Viral Proteins. Nano Lett. 2007; 7:3086–3091. [PubMed: 17894517]
3. Goldsmith BR, Coroneus JG, Khalap VR, Kane AA, Weiss GA, Collins PG. Conductance-Controlled Point Functionalization of Single-Walled Carbon Nanotubes. Science. 2007; 315:77–81. [PubMed: 17204645]
4. Chen RJ, Bangsaruntip S, Drouvalakis KA, Kam NWS, Shim M, Li YM, Kim W, Utz PJ, Dai HJ. Noncovalent Functionalization of Carbon Nanotubes for Highly Specific Electronic Biosensors. Proc. Nat. Acad. Sci. U. S. A. 2003; 100:4984–4989.

5. Staii C, Chen M, Gelperin A, Johnson AT. DNA-Decorated Carbon Nanotubes for Chemical Sensing. Nano Lett. 2005; 5:1774–1778. [PubMed: 16159222]
6. Zuniga C, Rinaldi M, Khamis SM, Johnson AT, Piazza G. Nanoenabled Microelectromechanical Sensor for Volatile Organic Chemical Detection. Appl. Phys. Lett. 2009; 94:223122.
7. Tang XW, Bansaruntip S, Nakayama N, Yenilmez E, Chang YL, Wang Q. Carbon Nanotube DNA Sensor and Sensing Mechanism. Nano Lett. 2006; 6:1632–1636. [PubMed: 16895348]
8. Zhou X, Moran-Mirabal JM, Craighead HG, McEuen PL. Supported Lipid Bilayer/Carbon Nanotube Hybrids. Nat. Nanotechnol. 2007; 2:185–190. [PubMed: 18654251]
9. Misra N, Martinez JA, Huang S-CJ, Wang Y, Stroeve P, Grigoropoulos CP, Noy A. Bioelectronic Silicon Nanowire Devices Using Functional Membrane Proteins. Proc. Nat. Acad. Sci. U. S. A. 2009; 106:13780–13784.
10. Huang S-CJ, Artyukhin AB, Misra N, Martinez JA, Stroeve PA, Grigoropoulos CP, Ju J-WW, Noy A. Carbon Nanotube Transistor Controlled by a Biological Ion Pump Gate. Nano Lett. 2010; 10:1812–1816. [PubMed: 20426455]
11. Filmore D. It's a GPCR World. Mod. Drug Discovery. 2004; 7:24–28.
12. Hulme, EC.; Birdsall, NJM. Receptor Biochemistry: A Practical Approach. Oxford, New York: IRL Press at Oxford University Press; 1990. p. xxi, 326
13. Raming K, Krieger J, Strotmann J, Boekhoff I, Kubick S, Baumstark C, Breer H. Cloning and Expression of Odorant Receptors. Nature. 1993; 361:353–356. [PubMed: 7678922]
14. Zhou XJ, Moran-Mirabal JM, Craighead HG, McEuen PL. Supported Lipid Bilayer/Carbon Nanotube Hybrids. Nat. Nanotechnol. 2007; 2:185–190. [PubMed: 18654251]
15. Bayburt TH, Grinkova YV, Sligar SG. Self-Assembly of Discoidal Phospholipid Bilayer Nanoparticles with Membrane Scaffold Proteins. Nano Lett. 2002; 2:853–856.
16. Graff RA, Swanson TM, Strano MS. Synthesis of Nickel-Nitrilotriacetic Acid Coupled Single-Walled Carbon Nanotubes for Directed Self-Assembly with Polyhistidine-Tagged Proteins. Chem. Mater. 2008; 20:1824–1829.
17. Kim TH, Lee SH, Lee J, Song HS, Oh EH, Park TH, Hong S. Single-Carbon-Atomic-Resolution Detection of Odorant Molecules Using a Human Olfactory Receptor-Based Bioelectronic Nose. Adv. Mater. 2009; 21:91–94.
18. Yoon H, Lee SH, Kwon OS, Song HS, Oh EH, Park TH, Jang J. Polypyrrole Nanotubes Conjugated with Human Olfactory Receptors: High-Performance Transducers for FET-Type Bioelectronic Noses. Angew. Chem., Int. Ed. 2009; 48:2755–2758.
19. Kajiya K, Inaki K, Tanaka M, Haga T, Kataoka H, Touhara K. Molecular Bases of Odor Discrimination: Reconstitution of Olfactory Receptors That Recognize Overlapping Sets of Odorants. J. Neurosci. 2001; 21:6018–6025. [PubMed: 11487625]
20. Saito H, Chi QY, Zhuang HY, Matsunami H, Mainland JD. Odor Coding by a Mammalian Receptor Repertoire. Sci. Signalling. 2009; 2:ra9.
21. Abaffy T, Matsunami H, Luetje CW. Functional Analysis of a Mammalian Odorant Receptor Subfamily. J. Neurochem. 2006; 97:1506–1518. [PubMed: 16606354]
22. Albert KJ, Lewis NS, Schauer CL, Sotzing GA, Stitzel SE, Vaid TP, Walt DR. Cross-Reactive Chemical Sensor Arrays. Chem. Rev. 2000; 100:2595–2626. [PubMed: 11749297]
23. Denisov IG, Grinkova YV, Lazarides AA, Sligar SG. Directed Self-Assembly of Monodisperse Phospholipid Bilayer Nanodiscs with Controlled Size. J. Am. Chem. Soc. 2004; 126:3477–3487. [PubMed: 15025475]
24. Bayburt TH, Sligar SG. Membrane Protein Assembly into Nanodiscs. FEBS Lett. 2010; 584:1721–1727. [PubMed: 19836392]
25. Bahr JL, Yang JP, Kosynkin DV, Bronikowski MJ, Smalley RE, Tour JM. Functionalization of Carbon Nanotubes by Electrochemical Reduction of Aryl Diazonium Salts: A Bucky Paper Electrode. J. Am. Chem. Soc. 2001; 123:6536–6542. [PubMed: 11439040]
26. Heller I, Janssens AM, Mannik J, Minot ED, Lemay SG, Dekker C. Identifying the Mechanism of Biosensing with Carbon Nanotube Transistors. Nano Lett. 2008; 8:591–595. [PubMed: 18162002]
27. Wise PM, Olsson MJ, Cain WS. Quantification of Odor Quality. Chem. Senses. 2000; 25:429–443. [PubMed: 10944507]

28. Schwende FJ, Wiesler D, Novotny M. Volatile Compounds Associated with Estrus in Mouse Urine - Potential Pheromones. Experientia. 1984; 40:213–215. [PubMed: 6538143]

29. Xu FQ, Schaefer M, Kida I, Schafer J, Liu N, Rothman DL, Hyder F, Restrepo D, Shepherd GM. Simultaneous Activation of Mouse Main and Accessory Olfactory Bulbs by Odors or Pheromones. J. Comp. Neurol. 2005; 489:491–500. [PubMed: 16025460]

30. Pevsner J, Trifiletti RR, Strittmatter SM, Snyder SH. Isolation and Characterization of an Olfactory Receptor Protein for Odorant Pyrazines. Proc. Nat. Acad. Sci. U. S. A. 1985; 82:3050–3054.

31. Furton KG, Myers LJ. The Scientific Foundation and Efficacy of the Use of Canines as Chemical Detectors for Explosives. Talanta. 2001; 54:487–500. [PubMed: 18968273]

32. Cox, C.; Weetjens, B.; Machangu, R.; Billet, M.; Verhagen, R. Rats for Demining: An Overview of The APOPO Program. Proceedings of the Eudem Conference on Humanitarian Landmine Detection Technologies; 2005. p. 5 pp

33. Zhang XM, Rogers M, Tian HK, Zhang XH, Zou DJ, Jian L, Ma MH, Shepherd GM, Firestein SJ. High-Throughput Microarray Detection of Olfactory Receptor Gene Expression in the Mouse. Proc. Nat. Acad. Sci. U. S. A. 2004; 101:14168–14173.

34. Wasilko DJ, Lee SE, Stutzman-Engwall KJ, Reitz BA, Emmons TL, Mathis KJ, Bienkowski MJ, Tomasselli AG, Fischer HD. The Titerless Infected-Cells Preservation and Scale-up (Tips) Method for Large-Scale Production of No-Sensitive Human Soluble Guanylate Cyclase (Sgc) from Insect Cells Infected with Recombinant Baculovirus. Protein Expr. Purif. 2009; 65:122–132. [PubMed: 19174191]

35. Sambrook, J.; Fritsch, EF.; Maniatis, T. Molecular-Cloning -a Laboratory Manual. Vol. Vol. 1. Cold Spring Harbor Laboratory Press; New York: 1989.

36. Ritchie TK, Grinkova YV, Bayburt TH, Denisov IG, Zolnerciks JK, Atkins WM, Sligar SG. Reconstitution of Membrane Proteins in Phospholipid Bilayer Nanodiscs. Methods Enzymol., Liposomes, Part F. 2009; 464:211–231.

37. Graff RA, Swanson TM, Strano MS. Synthesis of Nickel-Nitrilotriacetic Acid Coupled Single-Walled Carbon Nanotubes for Directed Self-Assembly with Polyhistidine-Tagged Proteins. Chem. Mater. 2008; 20:1824–1829.

38. Lu Y, Goldsmith BR, Kybert NJ, Johnson ATC. DNA-Decorated Graphene Chemical Sensors. Appl. Phys. Lett. 2010; 97:083107.

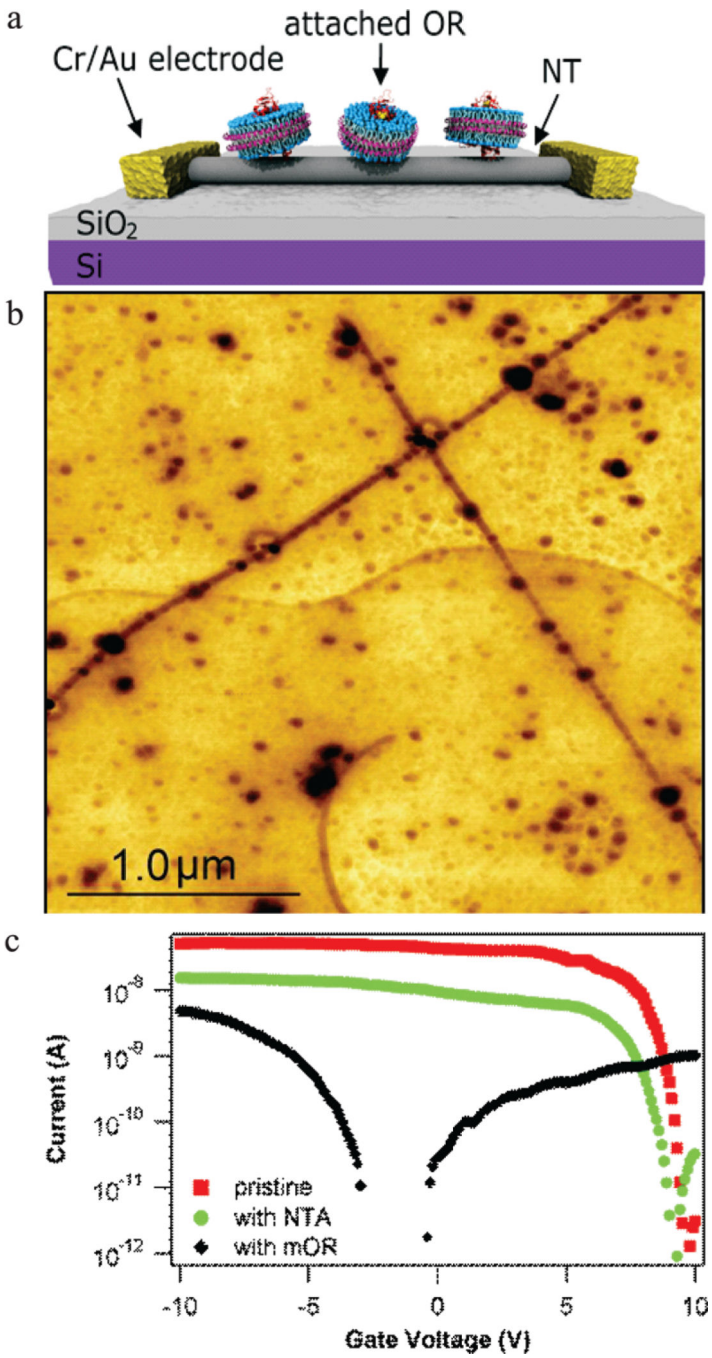

Figure 1.

Carbon nanotube devices functionalized with mouse olfactory receptor proteins (mORs). (a) Schematic of a carbon nanotube transistor functionalized with mORs in nanodiscs. (b) AFM image demonstrating preferential attachment of His-tag-labeled mOR 174-9 (darkest circles) in micelles to Ni-NTA-functionalized carbon nanotubes (dark lines). There is strong preference for attachment to the functionalized nanotubes compared to the background. (c) I–V_G curves of the same nanotube device as-fabricated (red), after Ni-NTA functionalization (green), and after incubation in a solution of mORs in digitonin micelles (black). The change

in $I–V_G$ associated with Ni-NTA functionalization is consistent with expectations based on association of Ni^{2+} atoms with NTA attached to the nanotube. The change in $I–V_G$ seen after mOR attachment is typical for protein functionalization of nanotube devices. Data were collected with a bias voltage of 100 mV.

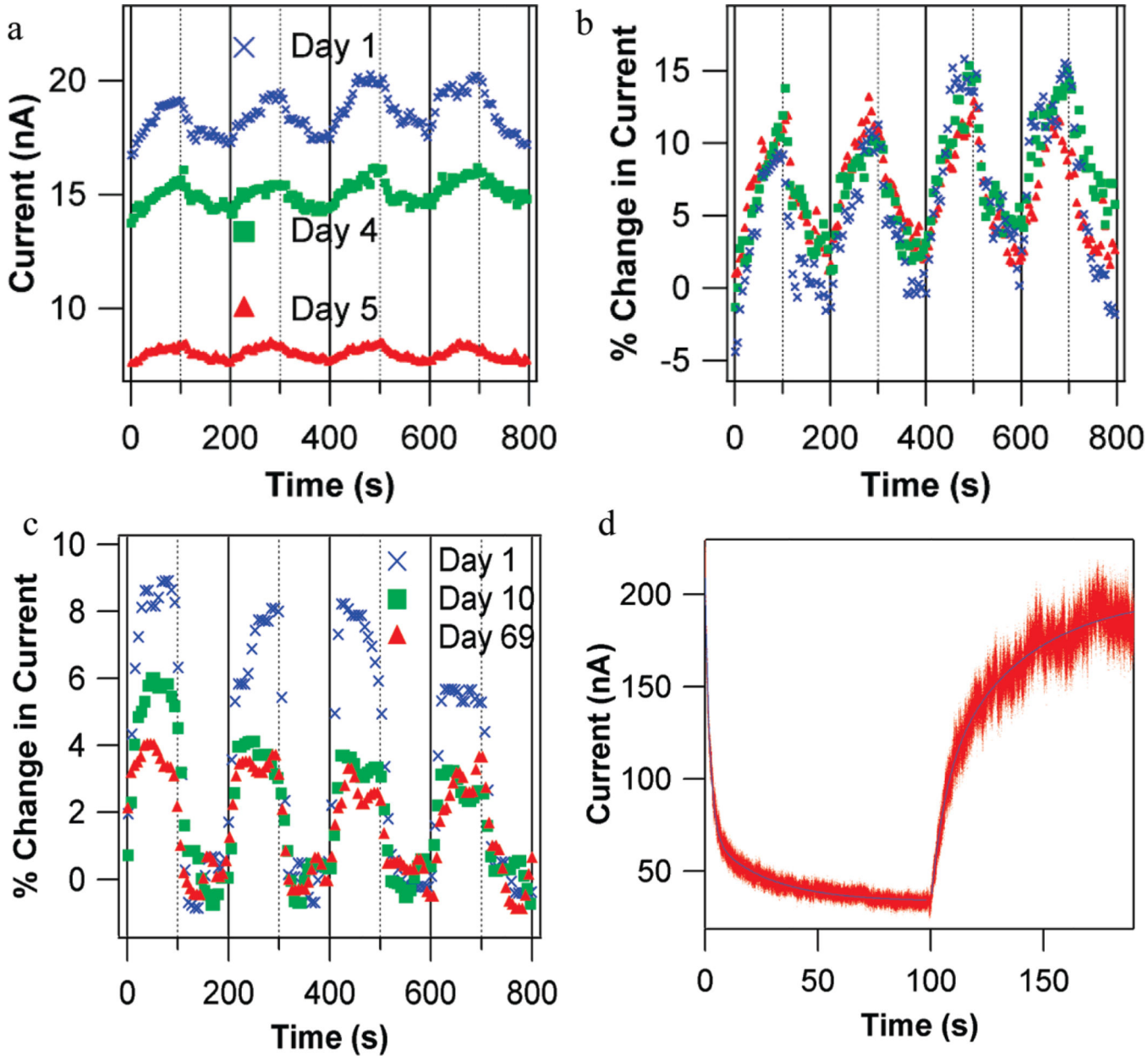

Figure 2.

Odorant responses of carbon nanotube (NT) devices functionalized with olfactory receptor proteins (ORs). (a) Three sets of responses to 2 ppm eugenol vapor taken over multiple days using a NT transistor functionalized with mOR174-9 in digitonin micelles. Eugenol vapor is introduced at time 0 and every 200 s (solid vertical lines). The chamber is flushed each time after 100 s of exposure (dashed vertical lines). Although the device baseline current shows significant drift over five days, the normalized current changes are identical, as seen in (b). (c) Characterization of nanodisc packaged OR-NT devices over 10 weeks. The device is based on mOR174-9 in nanodiscs, exposed to 2 ppm eugenol as described in (a). (d) Response to 2250 ppm cyclohexanone and recovery for a NT device functionalized with mOR 256-17 in nanodiscs, with 200 μs resolution. Flow of cyclohexanone begins at time =

0 s, and flow is replaced with clean N_2 at time = 100 s. Red points are raw data, and blue lines are fits based on double-exponential functions. Response time constants are 2.06 ± 0.1 and 25.51 ± 0.4 s. Recovery time constants are 6.49 ± 0.4 and 38.0 ± 0.2 s. NT device time scales are more rapid than those observed in heterologous expression systems (~2–10 min), where a cellular signal transduction pathway is used to report receptor activation.

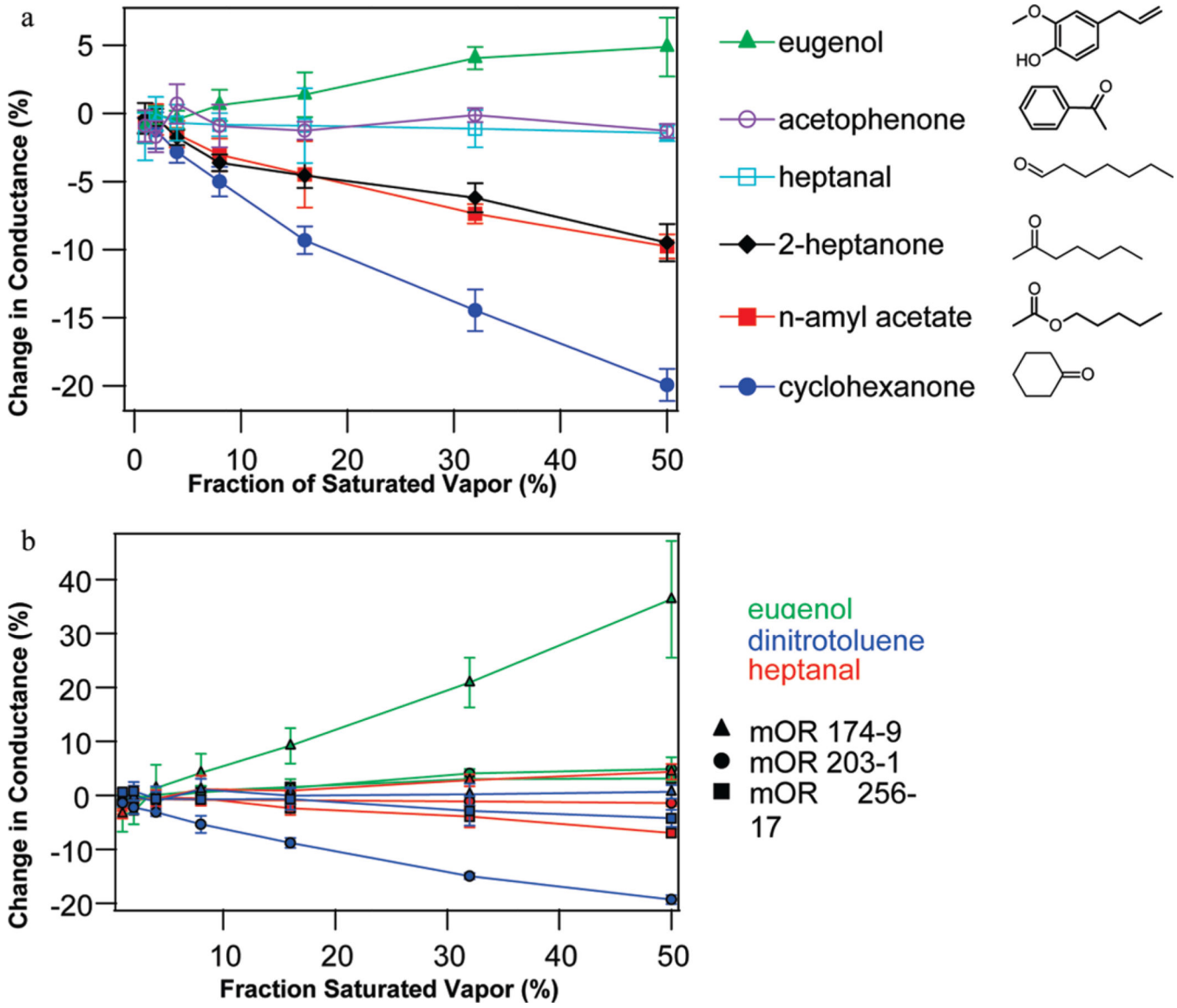

Figure 3.

Dependence of device responses upon mOR identity, odorant identity, and odorant concentration. (a) Concentration dependence of responses of NT devices functionalized with mOR203-1 in digitonin micelles to six different odorants. (b) Concentration dependence of the responses for NT devices functionalized with different mORs, tested against eugenol, 2,4-dinitrotoluene, and heptanal. The data demonstrate the diversity of chemical- and concentration-dependent responses seen in the mOR-NT system. Error bars are standard deviation.

TABLE 1

Responses of Mouse Olfactory Receptor Proteins (mORs) to Selected Odorants, in Biological and Electronic Systems[a]

	mOR 174-9			mOR 203-1			mOR 256-17			no OR	
	***Xenopus* oocyte**	**micelle nanotube**	**nanodisc nanotube**	**HEK**	**micelle nanotube**	**nanodisc nanotube**	***Xenopus* oocyte**	**micelle nanotube**	**nanodisc nanotube**	**empty micelle**	**bare NT**
eugenol	−8.4	+20.9±4.6	+7.2±1.1	0	+4.0\±0.8	+2.3±1.7	0	+3.0±0.8	+33.6±8.3	+0.5±1.3	0.0±0.2
2-heptanone	0	+4.1±2.2	−3.3±3.4	−4.76	−6.2±1.1	−6.5±1.5	−9.57	−10.5±0.8	−2.1±0.6	−0.7±0.5	+0.6±1.2
heptanal	0	+2.8±1.1	+5.4±3.1	0	−1.1±1.4	−2.2±0.9	−5.30	−3.9±2.0	−0.7±0.6	+1.7±1.7	+0.2±0.6
acetophenone	0	+6.1±0.8	−4.2±1.0	0	−0.1±0.5	−9.6±0.7	−5.93	+0.2±0.7	−2.3±0.8	+1.3±1.2	−0.1±0.1
2,4 DNT	0	+0.2±2.0	−7.7±1.2		−15.0±0.6	−0.7±2.0	−4.67	−2.9±2.7	−23.0±3.1	+0.1±0.7	+0.1±0.1
n-amyl acetate	0	0	−4.4±0.4		−7.4±0.7	−11.0±1.2	0	−16.5±1.0	−3.2±0.5	+0.9±1.4	+0.5±0.6
methyl benzoate	0	+5.6±1.9	−4.2±0.9		−0.9±1.9	−1.6±1.8	0	−3.9±0.8	+2.7±3.4	+0.3±0.6	+0.3±0.7
cyclohexanone	0	−28.2±1.6	−14.9±0.6	0	−14.4±1.5	−10.5±0.4	−1.00	−29.2±1.6	−35.3±3.9	+1.8±3.7	0.0±0.2

[a]For each type of experiment (*Xenopus* oocyte, HEK, and NT device), data are summarized in terms of relative sensing response. Blue indicates little or no response, red indicates a clear, strong response, and purple indicates a moderate response. White boxes represent biological data that are not available. HEK data are from ref 20. mOR-functionalized NT devices respond to odorants that elicit no response from bare NT devices or devices functionalized with empty micelles. Odorant sensitivities of mOR-functionalized NT devices vary with OR identity and are very similar to those seen in *Xenopus* and HEK experiments.